1-1-2013

Loss of dendritic inhibition in the hippocampus after repeated early-life hyperthermic seizures in rats.

Richard Boyce

L Stan Leung

Citation of this paper:

Boyce, Richard and Leung, L Stan, "Loss of dendritic inhibition in the hippocampus after repeated early-life hyperthermic seizures in rats." (2013). *Physiology and Pharmacology Publications*. 105.
https://ir.lib.uwo.ca/physpharmpub/105

journal homepage: www.elsevier.com/locate/epilepsyres

Loss of dendritic inhibition in the hippocampus after repeated early-life hyperthermic seizures in rats

Richard Boyce[a], L. Stan Leung[a,b,*]

[a] Department of Physiology and Pharmacology, University of Western Ontario, London, Ontario, Canada
[b] Program in Neuroscience, University of Western Ontario, London, Ontario, Canada

Summary   Seizures are relatively common in children and are a risk factor for subsequent temporal lobe epilepsy. To investigate whether early-life seizures themselves are detrimental to the proper function of the adult brain, we studied whether dendritic excitation and inhibition in the hippocampus of adult rats were altered after hyperthermia-induced seizures in immature rats. In particular, we hypothesized that apical dendritic inhibition in hippocampal CA1 pyramidal cells would be disrupted following hyperthermia-induced seizures in early life. Seizure rats were given three hyperthermia-induced seizures per day for three days from postnatal day (PND) 13 to 15; control rats were handled similarly but not heated. At PND 65—75, paired-pulse inhibition in area CA1 was evaluated under urethane anesthesia, using CA3 and medial perforant path (MPP) stimulation to excite the proximal and distal apical-dendrites, respectively, and the evoked field potentials were analyzed by current source density. There was no difference in the CA1 response to single-pulse stimulation of CA3 or MPP. In control rats, a high-intensity CA3 stimulus inhibited a subsequent MPP-evoked CA1 distal dendritic excitatory sink, and the inhibition at 150—200 ms was blocked by a $GABA_B$ receptor antagonist. Seizure as compared to control rats showed a decrease in a CA3-evoked inhibition of the CA1 distal dendritic excitation, 30—400 ms after the CA3 stimulus. In addition, seizure as compared to control rats showed a reduced early (20—80 ms) inhibition of a CA1 mid-apical dendritic sink following paired-pulse CA3 stimulation. In conclusion, long-term alterations in dendritic inhibition in CA1 were found following early-life seizures.
© 2012 Elsevier B.V. All rights reserved.

Introduction

Whether early life seizures have long-term functional conse-quences is controversial (Berg and Shinnar, 1997). Atypical, prolonged and recurrent febrile seizures in children may induce temporal lobe sclerosis (Falconer, 1974) and increase the risk of temporal lobe epilepsy (TLE) later in life

  * Corresponding author at: Department of Physiology and Phar-macology, Medical Sciences Bldg, University of Western Ontario, London, Canada N6A 5C1. Tel.: +1 519 850 2400; fax: +1 519 661 3827.
    E-mail address: sleung@uwo.ca (L.S. Leung).

(Annegers et al., 1987; Maher and McLachlan, 1995). How-ever, other epidemiological studies suggest that febrile seizures do not significantly increase the risk for the devel-opment of TLE or cognitive deficits without underlying neurological abnormalities (Nelson and Ellenberg, 1978; Verity and Golding, 1991; Verity et al., 1998).

Animal models provide insights into the consequences of seizure activity in the developing brain. As a model of febrile seizures, hyperthermia-induced seizures in immature rats (Baram et al., 1997) were found to increase long-term seizure susceptibility and induce spontaneous seizures (Dube et al., 2010), without significant cell loss or sustained brain damage (Dube et al., 2000). Additionally, long-term behavioral changes have been reported after hyperthermic seizures (Chang et al., 2003; Dube et al., 2000, 2009, 2010). Long-term physiological changes after febrile seizure mod-els include alteration of intrinsic membrane currents and an increased in $GABA_A$ receptor-mediated transmission in hippocampal slices *in vitro* (Chen et al., 1999). *In vivo*, a decreased $GABA_B$ receptor ($GABA_B$R)-mediated inhibition in CA1 was reported 30 days after repeated hyperthermia-induced seizures (Tsai and Leung, 2006) or early-life limbic seizures induced in immature rats (Tsai et al., 2008).

The primary purpose of the present study was to eval-uate the long-term effects of hyperthermic seizures on dendritic excitation and inhibition of CA1 pyramidal cells in rats *in vivo*. Specifically, we hypothesized that dendritic excitation and inhibition at the mid-apical and distal api-cal dendrites in CA1 are disrupted in rats that experienced early life seizures as compared to control rats. Repeated hyperthermic seizures were used as a model of early-life seizures, in particular for children with recurrent febrile seizures (Berg et al., 1997). Excitability following entorhi-nal cortex excitation of the CA1 distal apical dendrites was shown to be altered following status epilepticus in adult rats (Wu and Leung, 2003; Ang et al., 2006), but to our knowl-edge, synaptic transmission at the entorhinal-CA1 synapse *via* the medial perforant path (MPP) has not been studied following early-life seizures.

Methods

Subjects

All procedures were approved by the Animal Use Commit-tee at the University of Western Ontario (London, Ontario, Canada) and were conducted according to the guidelines set by the Canadian Council for Animal Care. Litters of imma-ture Long-Evans rats (9 days old) were acquired from Charles River, Quebec, Canada, and were kept with the mother in a 51 cm × 41 cm × 22 cm (width × length × height) Plexiglas cage until weaning on postnatal day 21. For the entire dura-tion of housing rats were given *ad libitum* access to food and water, and were kept on a 12 h:12 h light:dark cycle with lights on at 7:00 AM.

Repeated heated-air (hyperthermia)-induced seizures

On PND 13, male rats with similar weight were paired together, and each assigned pair was then arbitrarily divided

with one rat being placed in the hyperthermic seizure group and the other in the control group. Rats belonging to the seizure group were individually placed into a 3-l glass cylin-der which was partly immersed in a water bath kept at room temperature to help prevent overheating of the walking sur-face (Chang et al., 2003). A hair dryer at a moderate heat setting (500 W) was used to blow hot air down from the top of the container, ~50 cm above the head of the rat. The ambient air temperature within the container (measured at a height level with the rat's head) was kept between 46 and 49 °C (Chang et al., 2003). Temperature was measured by gentle insertion of a thermometer into the external ear canal before and after each hyperthermia/control session for every rat. In preliminary experiments, we monitored the relation between ambient, external ear and rectal temper-ature in rat pups of PND15. These data indicated that rectal temperatures of 38.4, 39.7, 41.4 and 42.7 °C were attained in 5, 10, 20 and 30 min of heating, respectively, with ambi-ent temperature reaching a plateau of 47 °C after 10 min of heating. External ear temperature was ~1 °C lower than rec-tal temperature. No recordings of brain temperature were performed in the rats that underwent hyperthermia treat-ment. In two pentobarbital anesthetized rat pups of similar age subjected to similar hyperthermia, the brain tempera-ture measured by a thermistor of 1 mm diameter inserted 2 mm into the sensorimotor cortex averaged 1.3 ± 0.1 °C higher than the rectal temperature during hyperthermia (38.4–42.2 °C rectal temperature). Thus, brain tempera-ture was estimated to be ~2.3 °C higher than external ear temperature. A hyperthermia-treated rat was kept in the container for 10 min following the first clearly observed behavioral seizure (typically hindlimb extension), or for a total duration of 30 min if no obvious seizure behavior was observed within the first 20 min of heating. Paroxys-mal electrical activity in the hippocampus and amygdala was previously recorded with the hyperthermia treatment in both our laboratory (Tsai and Leung, 2006) and the lab-oratory of others (Baram et al., 1997). The control rat was given similar treatment for the same duration as the seizure rat, except no heated air was applied. Upon com-pletion of a given session, the hyperthermic and control rats were returned to the home cage with the mother. In total, each hyperthermia and control rat underwent 3 hyperther-mic/control sessions per day (4 h between each session) for 3 consecutive days from PND 13 to 15. Following early life seizure treatment, small notches were cut in the ears of both control and seizure rats to allow for individual identi-fication later at the time of electrophysiological recording. A hyperthermia without seizure group was not used in the present study.

Surgical procedures

Approximately 50—60 days following early life treatment (PND 65—75), rats were put under urethane anesthesia (1.5 g/kg i.p.) and atropine methyl nitrate (0.15 mg/kg, i.p.) was injected to prevent fluid accumulation in the airway. Urethane anesthesia enhanced $GABA_A$ receptor inhibition and decreased glutamatergic excitation (Hara and Harris, 2002) but the entorhinal cortex to hippocampus circuit was preserved (Wu and Leung, 2003). After shaving the top of

its head, the rat was placed in a stereotaxic frame with ear bars. Normal body temperature was monitored by insertion of a rectal thermometer and maintained by a heating pad that was set for 36.7—36.9 °C. Once in the stereotaxic frame, an incision was made along the midline of the top of the head of the rat and the skull surface was exposed. The head position was then adjusted so that the lambda and bregma were level horizontally with one another. Jeweller's screws were placed in holes drilled through the anterior and posterior left quadrants of the skull to serve as ground and reference, respectively. Holes were drilled in the skull for insertion of a silicon recording probe and stimulating electrodes. The silicon probe had 16 electrodes at 50 μm intervals on a vertical shank (Neuronexus, Ann Arbor, MI; 5 mm long shank and 177 μm^2 recording surface), covering a vertical distance of 750 μm. It was inserted vertically into the right CA1 (P 3.8, L 2.5 with respect to bregma, Paxinos and Watson, 1986; Fig. 1A and B). Stimulating electrodes (~0.2 mm diameter Teflon insulated stainless steel wires) were lowered to stimulate the MPP (P 8.0, L 4.4) or CA3 region (P 3.2, L 3.3), which evoked distal and mid-apical dendritic excitation of CA1 pyramidal neurons, respectively (Fig. 1). Following the lowering of electrodes, the brain was allowed to recover for at least 1 h to ensure stability of recordings.

Electrophysiological recordings

Signals from the silicon probe were amplified 200—1000× by a preamplifier and amplifier (Tucker Davis Technology, FL) and sampled at 12 kHz. Single and average evoked potentials (four sweeps averaged) were stored by a custom program.

Single or paired stimulus pulses were delivered at 10 s intervals to the CA3 or MPP electrode. Paired-pulses were either homosynaptic (both pulses delivered through the same electrode) or heterosynaptic (one pulse from each electrode; first pulse = unconditioned, second pulse = conditioned), resulting in four conditions — two homosynaptic, CA3—CA3 and MPP—MPP; and two heterosynaptic, CA3—MPP and MPP—CA3. To obtain input—output data CA1 test pulse responses were recorded at various stimulus intensities ranging from 30 to 500 μA, with a fixed interpulse interval (IPI) of 50 or 200 ms for paired-pulse stimuli. IPI profiles were created by varying the delay between pulses from 20 to 400 ms while keeping the intensity of stimuli fixed; CA3 stimulation was adjusted to evoke ~70% of the maximal population spike (PS) in CA1, and MPP stimulation was adjusted to evoke ~70% of the maximal PS in the dentate gyrus or near maximal MPP-evoked distal dendritic sinks in CA1 (Leung et al., 1995). The IPI was varied to help differentiate between an early ionotropic GABA$_A$ receptor-mediated inhibition at <100 ms (Steffensen and Henriksen, 1991) and a metabotropic GABA$_B$ receptor-mediated inhibition at >100 ms (Tsai and Leung, 2006; Olpe et al., 1993; Isaacson et al., 1993).

In some experiments, the effect of the specific GABA$_B$R antagonist 3-amino-propyl-diethoxymethyl-phosphinic acid (CGP35348) on heterosynaptic paired-pulse responses was studied. A 23-gauge outer cannula was placed over the lateral ventricle (P 0.8, L 1.4, V 4.6), and baseline recordings were made. At the time of injection, 93 μg (400 nmol) of CGP35348 dissolved in 1.33 μl of saline was injected
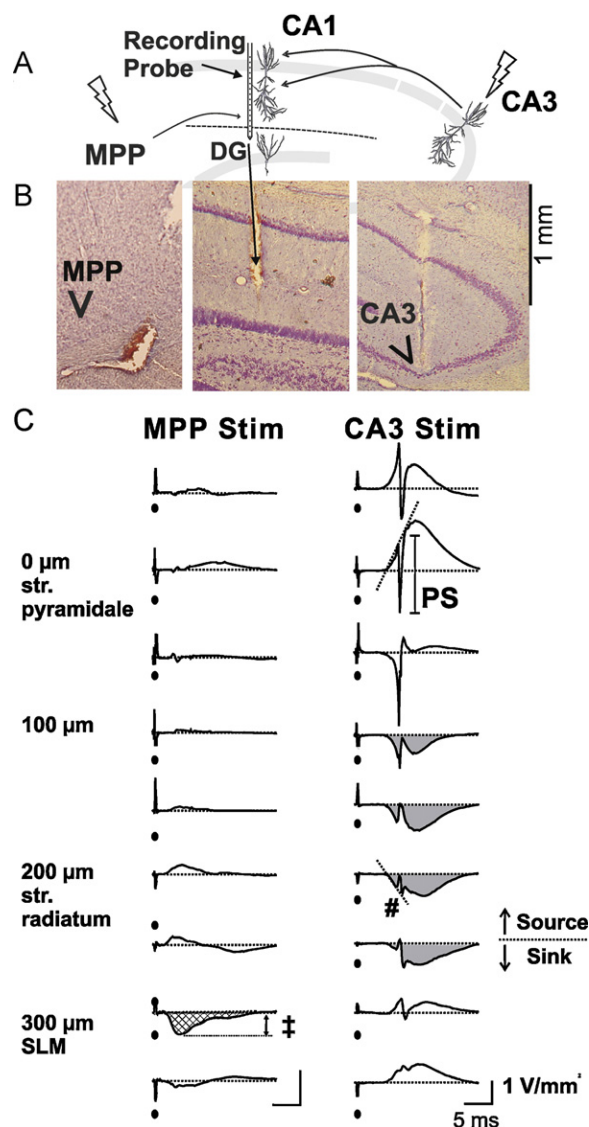
Figure 1 Current source density (CSD) temporal responses in hippocampal CA1 following medial perforant path (MPP) and CA3 stimulation, analyzed from average evoked potentials (4 sweeps). (A) Schematic diagram of stimulus and recording electrodes, with (B), representative thionin-stained coronal sections showing typical location of the stimulating electrode in MPP (leftmost) and CA3 (rightmost), and silicon recording probe in CA1 (center). (C) Laminar profiles of CSDs in CA1 evoked by MPP and CA3 stimulation. Following MPP simulation, an excitatory sink can be seen at the distal apical dendrites (hatched fill) in stratum lacunosum-moleculare (SLM), with an accompanying source in stratum (str.) radiatum. The distal dendritic sink was measured by the negative peak amplitude relative to baseline (‡). A moderately high-intensity CA3 stimulation (traces at right) evoked excitatory sinks in stratum radiatum (shaded gray), flanked by current sources at the pyramidal cell layer (str. pyramidale) and SLM, and a sharp population spike (PS) sink near str. pyramidale. PS was measured by its amplitude to a tangent line linking the positive peaks, and the CA3-evoked str. radiatum sink was measured by the maximally negative slope (over 1 ms duration) during the rising phase (#), before the onset of the PS. Black circle indicates stimulus artifact.

intracerebroventricularly (icv) by a 26-gauge cannula into the lateral ventricle.

Data analysis

Average evoked field potentials recorded during paired-pulse stimulation were subjected to a one-dimensional current source density (CSD) analysis, the inverse process of deriving the current sources and sinks that generate a field potential by eliminating volume conduction (Freeman and Nicholson, 1975; Leung, 2010). Since the cellular current generators — CA1 pyramidal cells — are lined up in palisades, their sum current is mainly along the longitudinal axis of the cells. Thus, a one-dimensional CSD analysis estimates the current sources and sinks in depth, as described by the equation

$$CSD(z, t) = \frac{\sigma[2\varphi(z, t) - \varphi(z + \Delta z, t) - \varphi(z - \Delta z, t)]}{(\Delta z)^2},$$

where $\varphi(z,t)$ is the potential at depth z and time t, and Δz (50 μm) is the space between adjacent electrodes on the silicon probe. No smoothing of CSD and potential was necessary for silicon probe recordings. The conductivity σ was assumed to be constant, and the CSDs are reported in units of V/mm^2.

Following CA3 stimulation, the Schaffer collaterals (axons of CA3 pyramidal cells) excite the apical dendrites of CA1 pyramidal cells, generating a population excitatory postsynaptic potential (pEPSP) that was negative at stratum radiatum and positive at the pyramidal cell layer. CSD analysis revealed an excitatory current sink (inward current) in stratum radiatum (Leung, 2010), flanked by current sources in the pyramidal cell layer and stratum lacunosum-moleculare (SLM, or layer of the distal apical dendrites). A high CA3 stimulus intensity evoked a PS in CA1, which corresponds to synchronous action potentials of CA1 pyramidal cells. CSD analysis of the PS revealed a sharp current sink at the pyramidal cell layer with an accompanying current source in the apical dendrites (Leung, 2010). MPP stimulation excited the distal apical dendrites of CA1 pyramidal cells. CSD analysis revealed a current sink in the SLM of CA1, with an accompanying current source in CA1 stratum radiatum (Leung et al., 1995; Wu and Leung, 2003).

The PS in CA1 resulting from CA3 stimulation was measured by the amplitude of the PS sink at the CA1 pyramidal cell layer. A tangent line was extrapolated to join the positive peaks before and after the PS sink, and the PS sink amplitude was measured as the vertical distance between the minimum sink to the tangent line (PS in Fig. 1C). The CA3-evoked excitatory sink was measured by determining the maximally negative slope, over 1 ms duration, from the rising phase of the pEPSP sink in stratum radiatum, before the onset of the PS (# in Fig. 1C). In seizure and control rats, the MPP evoked CA1 distal dendritic excitation was measured by determining the maximal amplitude of the sink at SLM relative to the pre-MPP stimulus baseline (‡ in Fig. 1C). For recordings made before and after icv CGP35348, the SLM sink was assessed at 4.5—7.5 ms after a MPP stimulus (fixed for each rat), relative to the baseline at 0.1 ms immediately before the MPP stimulus. The latter procedure is necessary for excluding the polysynaptic activity in CA1 induced by icv CGP35348 (below), and it measured the putatively mono-synaptic SLM sink before its peak during no-drug condition (Leung et al., 1995). In all recordings, the CA1 pyramidal cell layer was assumed to be the location of the maximal PS sink, and the location of the distal source associated with the CA3-evoked pEPSP corresponded to the location of the maximal excitatory sink evoked by the MPP stimulus in SLM. Distance between the pyramidal cell layer and SLM could be confirmed by the histology of the CA1 area with the track of the silicon probe (Fig. 1B).

Paired-pulse responses were calculated as the ratio of the conditioned/unconditioned (C/UC) response, where a value greater than 1 indicated paired-pulse facilitation, while a value less than 1 indicated paired-pulse inhibition.

Histology

At the end of the experiment, rats were perfused through the heart with 50 ml of 0.9% saline solution followed by 50 ml of 4% buffered formaldehyde solution. Brain sections 40-μm thick were cut using a freezing microtome and subsequently stained with thionin for verification of recording probe and electrode locations (Fig. 1B).

Statistics

Statistical significance was evaluated by repeated measures analysis of variance (ANOVA), followed by *post hoc* Newman—Keuls tests. Data are presented as mean $\pm$ standard error of the mean (SEM). $p < 0.05$ was considered statistically significant.

Results

Hyperthermia-induced seizures

The following results were obtained from 11 male rats that underwent hyperthermia treatment (3 hyperthermia sessions per day for 3 days for a total of 9 hyperthermia sessions) to induce seizures at PND 13—15, along with 11 control rats. In the hyperthermia-treated rats ($n = 11$), the external ear temperature was 35.8 ± 0.1 °C immediately prior to heating and 38.4 ± 0.1 °C at the conclusion of the hyperthermia treatment. Brain temperature during hyperthermia was estimated to be ~2.3 °C higher than external ear temperature (Methods). Immobility or freezing behavior typically began after about 7 min of hyperthermia, followed later by seizure behaviors that included myoclonic jerks (48.5% of heating sessions), and immobility with tonic—clonic movement (28.3% of heating sessions). The likelihood of the occurrence of two seizure behaviors, myoclonic jerks and tonic—clonic movements, increased with the three seizures evoked on the same day except for myoclonic jerks on the third day of treatment, but there was no evidence of seizure progression day after day (Fig. 2). Each hyperthermia-treated rat demonstrated myoclonic jerks and all but one rat demonstrated overt tonic—clonic movements at least once during the course of 9 hyperthermia sessions. Rats were subjected to hyperthermia for an average duration of
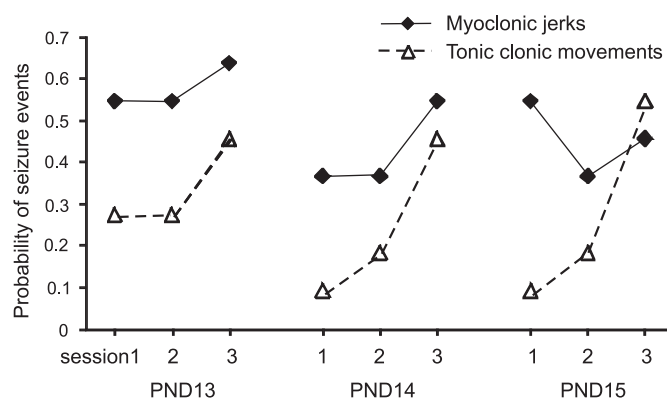
Figure 2   Probability of occurrence of seizure events during the heating sessions, three per day for 3 consecutive days (PND13—PND15). Two seizure events, myoclonic jerk and tonic—clonic movement, were scored as present or not during each heating session, with sessions separated by 4 h on each day. Each session resulted in 0.1—0.65 probability of inducing a particular seizure event. The probability of seizure event increased with the three seizures induced on the same day, except for myoclonic jerks on PND15, but not day after day.

29.1 $\pm$ 0.3 min per session, which was highly uniform regardless of treatment day or hyperthermia session within a treatment day. No control rats showed any indication of seizure-like behavior. No mortality was associated with the hyperthermia treatment utilized in this study.

CA1 response following single pulse stimulation

Electrophysiological responses were recorded in hyperthermia-treated (seizure) and control rats at 50—60 days after seizure/control treatment. The input—output curves of single-pulse stimulation responses in CA1 evoked by CA3 or MPP were not different between seizure and control rats. Measurements included the amplitude of the PS sink at the CA1 cell layer evoked by a single CA3 stimulus ($F_{1,16} = 0.14$, $p = 0.71$ for group effect; Fig. 3A), the magnitude of the CA3-evoked apical dendritic sink at 200 μm from the CA1 cell layer ($F_{1,14} = 0.08$, $p = 0.82$ for group effect; Fig. 3B) or 250 μm from the CA1 cell layer ($F_{1,11} = 0.70$, $p = 0.42$ for group effect; data not shown), and the MPP-evoked distal dendritic sink ($F_{1,7} = 0.01$, $p = 0.99$ for group effect; Fig. 3C) in seizure relative to control rats, all with non-significant group $\times$ intensity interaction.

## Homosynaptic paired-pulse responses in CA1

Homosynaptic paired-pulses (CA3—CA3) were delivered at varying IPIs to area CA3 to assess the paired-pulse responses at the CA1 cell layer and mid-apical dendrites (stimulus intensity: seizure rats 222 $\pm$ 24 μA, control rats 175 $\pm$ 23 μA). The CA3-evoked PS at the CA1 pyramidal cell layer showed no difference in the C/UC ratio between seizure and control rats at any of the IPIs tested [$F_{1,20} = 0.02$, $p = 0.88$ for group (seizure *versus* control) effect; $F_{7,140} = 0.11$, $p = 0.99$ for group $\times$ IPI interaction (7 levels of IPI from 30 to 400 ms); Fig. 4A]. In contrast, at the mid-apical dendrites ~200 μm from the pyramidal cell layer, the C/UC ratio of the evoked apical dendritic sink was significantly higher in seizure than control rats at 20—80 ms IPIs ($F_{1,17} = 6.25$, $p = 0.02$ for group effect;

$F_{7,119} = 3.52$, $p < 0.01$ for group $\times$ IPI interaction; Fig. 4B). At a more distal dendritic site, ~250 μm from the pyramidal cell layer, the C/UC ratio of the evoked excitatory sink was not different between seizure and control rats ($F_{1,15} = 0.40$; $p = 0.54$ for group effect; $F_{7,105} = 0.32$; $p = 0.72$ for group $\times$ IPI interaction; data not shown).

The homosynaptic paired-pulse response at the CA1 distal apical dendrites was evaluated by delivering paired pulses (seizure 200 $\pm$ 34 μA, control 200 $\pm$ 22 μA) to the MPP at various IPIs. The C/UC ratio of the MPP-evoked CA1 distal apical dendritic excitatory sink was not different between seizure and control rats ($F_{1,9} = 0.39$; $p = 0.55$ for group effect; $F_{7,63} = 0.64$; $p = 0.72$ for group $\times$ IPI interaction; Fig. 4C).

Heterosynaptic paired-pulse responses in CA1

In order to assess the effect of MPP evoked inhibition on CA3-evoked responses, a conditioning pulse was delivered to MPP at an intensity that evoked ~70% of the maximal PS in the dentate gyrus, followed at an IPI of 20—400 ms, by a pulse delivered to CA3 at a stimulus intensity capable of evoking 70% of the maximal PS in CA1. There was no significant difference between seizure and control rats in either the MPP stimulus intensity (250 $\pm$ 23 μA in both groups) or the CA3 stimulus intensity (seizure rats 223 $\pm$ 24 μA, control rats 175 $\pm$ 23 μA) used. The C/UC ratio of the CA3-evoked PS sink at the CA1 pyramidal cell layer was not significantly different between seizure and control rats ($F_{1,20} = 1.17$; $p = 0.29$ for group effect; $F_{7,140} = 0.45$; $p = 0.87$ for group $\times$ IPI interaction; data not shown). In contrast, the C/UC ratio of the CA3-evoked excitatory sink at the CA1 mid-apical dendrites, located ~200 μm from the pyramidal cell layer, was significantly higher at 30 ms IPI in seizure rats relative to control rats ($F_{1,17} = 0.38$; $p = 0.55$ for group effect; $F_{7,119} = 2.20$; $p = 0.04$ for group $\times$ IPI interaction; Fig. 5A). At ~250 μm from the pyramidal cell layer, the C/UC ratio of the evoked excitatory sink was not different between seizure and control rats ($F_{1,14} = 3.98$; $p = 0.07$ for group effect; $F_{7,98} = 1.16$; $p = 0.33$ for group $\times$ IPI interaction; data not shown).
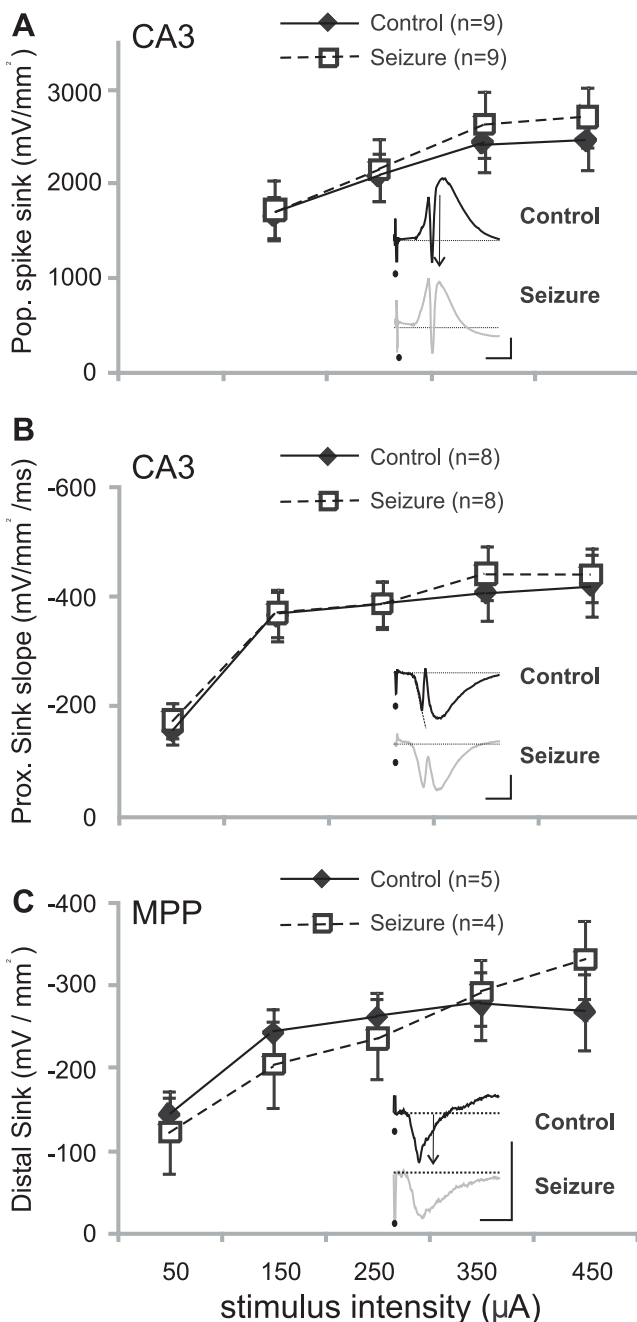
Figure 3 Single-pulse excitatory sink responses (mean ± SEM) in CA1 as a function of stimulus intensity were not significantly different between control and seizure rats. (A) Population spike sink amplitude measured at the pyramidal cell layer, (B) excitatory sink at the proximal apical dendrites ~200 μm from the pyramidal cell layer following CA3 stimulation, and (C) distal apical dendritic excitatory sink amplitude following MPP stimulation. Recordings were made ~50 days after control or hyperthermic seizure treatment. Representative traces at 250 μA are shown for control (dark) and seizure (gray) rats. Black circle indicates stimulus artifact. Scale bars represent 0.5 V/mm² vertically and 5 ms horizontally.

Heterosynaptic paired-pulse inhibition of the CA1 distal apical dendritic sink was evaluated by delivering a conditioning stimulus to CA3 followed 30—400 ms later by a MPP pulse. In control rats, the MPP-evoked distal dendritic sink showed a detectable suppression only when the CA3 stimulus exceeded PS threshold in CA1 (Fig. 5B1). However, the suppression of the MPP-evoked distal dendritic sink did not depend on MPP stimulus intensity (Fig. 5B2). Therefore both seizure and control rats were given a CA3 stimulus intensity that evoked ~70% of the maximal evoked PS in CA1 (seizure 283 ± 42 μA, control 290 ± 40 μA) followed by a test pulse to MPP at an intensity that evoked ~70% of the maximal PS in the dentate gyrus (seizure 183 ± 42 μA, control 210 ± 24 μA). The C/UC ratio of the MPP-evoked distal apical dendritic sink was significantly greater in seizure rats than control rats at all IPIs tested ($F_{1,9} = 11.28$, $p = 0.01$ for group effect; $F_{6,54} = 0.92$, $p = 0.49$ for group × IPI interaction; Fig. 5C).

In order to test the participation of GABA$_B$ receptors in the suppression of the MPP-evoked distal dendritic sink by a CA3 conditioning stimulus, heterosynaptic CA3—MPP paired-pulse responses were recorded before and after icv infusion of GABA$_B$R antagonist CGP35348. During baseline before icv infusion, the conditioned distal dendritic response in CA1 showed paired-pulse depression at short (<80 ms) and long (>100 ms) IPIs (Fig. 6A). After icv CGP35348, the depression at long IPIs was reduced (two-way repeated measured ANOVA, significant group × IPI interaction effect $F_{6,24} = 3.5$, $p < 0.02$, without a significant group effect). *Post hoc* Newman—Keuls test revealed significant differences ($p < 0.05$) at IPI of 150 and 200 ms (Fig. 6A). Representative traces show that the conditioned SLM distal dendritic sink at 4—7 ms latency (arrow in Fig. 6B) was increased after CGP35348 as compared to baseline. However, at 8—25 ms latency, a source in SLM (# in Fig. 6B) developed in correspondence to a stratum radiatum excitatory sink and a PS in CA1, likely mediated polysynaptically through CA3 (Leung et al., 1995). CGP35348 also increased, as compared to baseline, a mid-dendritic excitatory sink and PS in the dentate gyrus (DG PS in Fig. 6B) evoked by a MPP stimulus. However, icv CGP35348 did not significantly alter the PS evoked by the conditioning CA3 stimulus, or the distal CA1 sink evoked by a non-conditioned MPP stimulus.

Discussion

CSD analysis revealed no alteration in the single-stimulus-pulse evoked excitation of the mid-apical or distal apical dendrites in hippocampal CA1 after repeated hyperthermia-induced seizures as compared to control rats. However, paired-pulse inhibition of a proximal apical dendritic excitation in stratum radiatum was reduced at 20—80 ms latencies, and CA3-evoked inhibition of distal apical dendritic excitation was reduced at 30—400 ms latencies in seizure rats as compared to controls. The data suggest that dendritic inhibition in CA1 was disrupted by early-life seizure activity.

Long-lasting loss of CA1 proximal dendritic inhibition after early-life hyperthermic seizures

In the present study, immature rats of PND 13—15 typically began to show abnormal behaviors after ~7 min of heating.
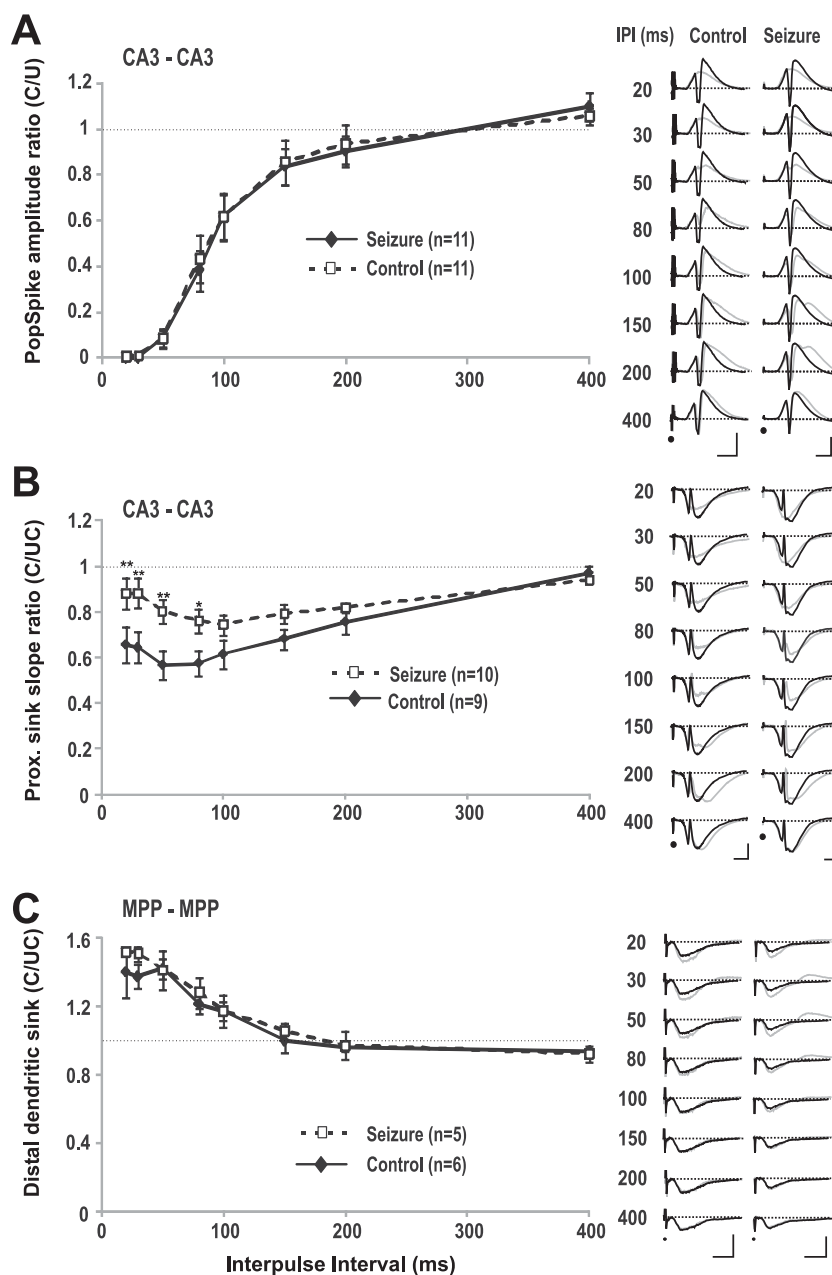
Figure 4 CA3 and medial perforant path (MPP) evoked homosynaptic paired-pulse responses (mean ± SEM) at different interpulse intervals (IPIs) recorded in adult rats following control or hyperthermic seizure treatment. (A) The homosynaptic ratio of the CA1 population spike sink amplitude (at the cell layer) evoked by the second CA3 pulse to that evoked by the first CA3 pulse (conditioned/unconditioned response ratio, or C/UC) between control and seizure rats was not different at any of the IPIs tested. (B) The C/UC ratio of the proximal apical dendritic excitatory sink ∼200 μm from CA1 cell layer following homosynaptic CA3 stimuli was significantly larger in seizure compared to control rats at IPIs of 20–80 ms. (C) The C/UC ratio of the CA1 distal apical dendritic sink following paired-pulse homosynaptic MPP stimuli was not different between control and seizure rats at any of the IPIs tested. *$p < 0.05$, **$p < 0.01$, *post hoc* Newman–Keuls test after repeated measures ANOVA. Representative traces showing UC (dark) traces overlying C (light) responses are shown on the right. Black circle indicates stimulus artifact. Scale bars represent 0.5 V/mm^2 vertically and 5 ms horizontally.

These behaviors included initial prolonged immobility that was accompanied by myoclonic jerks and tonic–clonic movements as the hyperthermia session progressed. No EEG recordings were made in the present study, but in previous studies, epileptiform EEG activities were shown in the hippocampus and amygdala using hyperthermia duration similar to the present study (Baram et al., 1997; Tsai and Leung, 2006).

In adult rats (PND 65–75), two main differences in dendritic inhibition were found between seizure and control
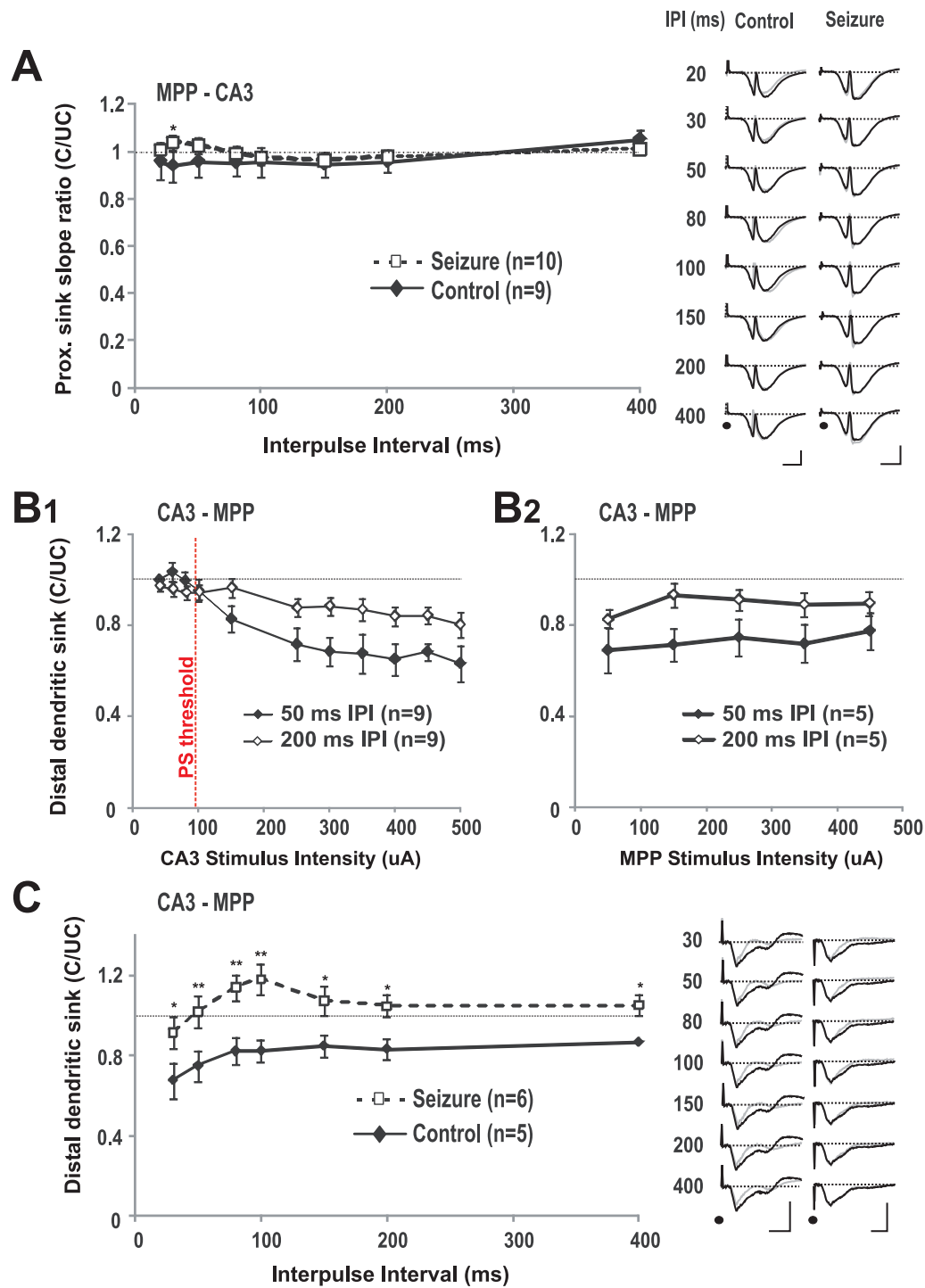
Figure 5 Heterosynaptic paired-pulse responses (mean ± SEM) at different interpulse intervals (IPIs) recorded in adult rats following control or hyperthermic seizure treatment. (A) The conditioned/unconditioned response ratio (C/UC) of the proximal apical dendritic excitatory sink evoked by CA3 stimulus ~200 μm from the CA1 cell layer shows a significantly higher suppression by the MPP conditioning pulse in seizure rats than control rats at 30 ms IPI. (B1) A CA3 conditioning pulse suppressed the MPP-evoked distal dendritic sink at CA3 stimulus intensities capable of evoking a CA1 population spike (PS); IPIs of 50 and 200 ms were used. The vertical dotted line at 97 μA (±11 μA) indicates the mean (±SEM) threshold intensity for evoking a PS. (B2) At a fixed CA3 stimulus intensity that evoked 70% of the maximal PS, the C/UC ratio was not affected by MPP stimulus intensity. (C) The C/UC ratio at 30−400 ms IPI shows that a CA3 conditioning pulse (that evoked 70% of the maximal PS in CA1) suppressed the MPP-evoked distal dendritic sink significantly more in control rats than seizure rats. *$p < 0.05$, **$p < 0.01$, *post hoc* Newman−Keuls test after repeated measure ANOVA. For figures A and C representative traces showing UC (dark) traces overlying C (light) responses are included at right. Black circles indicate stimulus artifact. Scale bars represent 0.5 V/mm^2 vertically and 5 ms horizontally.
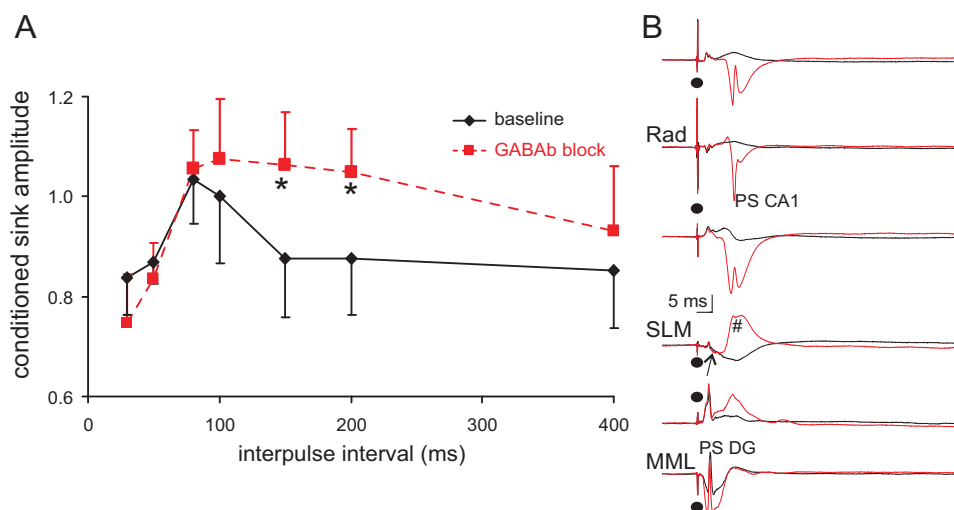
Figure 6 Heterosynaptic paired-pulse responses (mean ± SEM) at different interpulse intervals (IPIs) recorded before (baseline) and after intracerebroventricular (icv) infusion of 400 nmol of CGP35348. (A) Group data ($n = 5$) showing ratio of conditioned sink amplitude at the distal dendrites of CA1 (stratum lacunosum-moleculare, SLM) at different IPIs, during baseline and after CGP35348. For each rat, the conditioned sink amplitude was normalized by the absolute amplitude of the non-conditioned sink evoked by a single MPP stimulus during baseline. CGP35348 (icv) did not significantly alter the normalized conditioned sink amplitude at 30—100 ms IPI, but it significantly increased the conditioned sink amplitude at 150 and 200 ms IPI. (B) Representative traces of the MPP evoked CSD transients in CA1 plotted at 100 μm intervals, at 200 ms IPI after a CA3 conditioning pulse. After GABA_B receptor blockade by icv CGP35348 as compared to baseline, the SLM early sink (arrow) and the middle molecular layer (MML) sink in the dentate gyrus (DG) was larger, and a large SLM source (8—25 ms latency) followed the early SLM sink. The latter SLM source occurs at the time of a stratum radiatum (RAD) mid-apical dendritic sink that resulted in a population spike (PS) in CA1. Black circle indicates stimulus artifact.

rats. First, there was a decrease in the inhibition (20—80 ms) of the CA1 proximal apical dendritic excitatory sink evoked by paired-pulse stimuli to CA3, and second, a decrease in CA3-evoked inhibition (at latencies of 30—400 ms) of the MPP-evoked distal dendritic excitation in CA1.

At the proximal CA1 apical dendrites, ~200 μm from the pyramidal cell layer, control rats showed a CA3—CA3 paired-pulse response ratio (C/UC) of less than unity for the range of IPI (20—400 ms) tested (Fig. 4B), confirming the paired-pulse inhibition of the proximal apical dendritic sinks reported previously (Leung et al., 2008). In the present study, we showed that the paired-pulse inhibition ratio (C/UC) at the proximal dendrites was significantly reduced in seizure compared to control rats at 20—80 ms IPI. Since the first-pulse (UC) response to CA3 stimulation was not different between seizure and control rats (Fig. 3B), the difference in ratio must be attributed to the second-pulse (C) response. Decreased inhibition of the CA3-evoked proximal apical dendritic sink by a MPP conditioning pulse (Fig. 5A) also suggests a similar loss of proximal apical dendritic inhibition in seizure as compared to control rats. Previous study in our laboratory (Leung et al., 2008) showed that paired-pulse inhibition of the proximal apical dendritic sinks evoked by CA3 homosynaptic paired-pulse stimulation was blocked by GABA_A receptor antagonist picrotoxin, suggesting a post-synaptic GABA_A receptor-mediated inhibition (Steffensen and Henriksen, 1991), possibly by basket cells (Freund and Buzsaki, 1996; Leung et al., 2008). However, the lack of CA1 PS inhibition suggests a layer-specific re-distribution of

inhibition, but not a decrease in total inhibition of spike firing. Layer-specific presynaptic alteration of the conditioned *versus* non-conditioned excitation of the proximal dendrites cannot be excluded.

In a previous *in vitro* study, hyperthermic seizures in immature rats were shown to result in a long-lasting (up to 10 weeks post-seizure) increase in a GABA_A receptor-mediated somatic inhibition in CA1 neurons in horizontal hippocampal slices (Chen et al., 1999). Chen et al. (1999) reported a decrease in CA1 PS amplitude evoked by single pulse stimulation of the Schaffer collaterals in seizure as compared to control rats. We (Tsai and Leung, 2006; this study) did not find single-pulse PS amplitude change. In addition, we did not infer an increase in short-latency, presumably GABA_A receptor-mediated, inhibition in hyperthermia-seizure rats as compared to control rats. However, the inhibition reported by Chen et al. (1999) was likely derived from whole cell somatic patch, and not from dendritic membrane. In addition, based on a model simulating both intracellular and field responses of CA1 pyramidal cells (Leung and Peloquin, 2006), while a change in the H-current characteristics after seizures may alter spike excitability (Chen et al., 2001), it does not account for the difference in heterosynaptic paired pulse response in seizure compared to control rats as shown in Fig. 5C (simulation data not shown). Other than a difference in the age of seizure induction (PND 10 in Chen et al., 1999; PND 13—15 in the present study), a decrease in inhibition *in vitro* (Buckmaster and Schwartzkroin, 1995) and an

increase under urethane anesthesia (Hara and Harris, 2002) as compared to an awake animal, may contribute to the difference in GABA$_A$ inhibition results. The present study, in which recordings were made 50 days after hyperthermic seizures, found no change in the late (presumably GABA$_B$-receptor mediated) paired-pulse inhibition of the PS at the CA1 cell layer, as compared to a late paired-pulse inhibition decrease reported 14 days after seizures (Tsai and Leung, 2006).

Reduction of CA1 distal dendritic inhibition after hyperthermic seizures

The heterosynaptic (CA3—MPP) paired-pulse inhibition of the distal dendritic sink was significantly reduced at all IPIs (30—400 ms) in seizure rats as compared to control rats (Fig. 5C). In control rats, CA3—MPP paired-pulse inhibition was indicated by a C/UC ratio of less than unity at all IPIs, while in seizure rats, paired-pulse facilitation was indicated by a C/UC ratio above unity at IPI > 30 ms. Since CA1 responses to single-pulse stimulation of CA3 or MPP were not different between seizure and control rats, the difference in paired-pulse response suggest a decrease in inhibition, or an increase in paired-pulse facilitation, of the distal dendritic response in seizure as compared to control rats. Inference of distal dendritic inhibition by means of the amplitude of an excitatory sink in the present study is an indirect method, and can be compared with inference of presynaptic inhibition in central synapses. However, direct patch or intracellular recordings from the distal dendrites in SLM was difficult *in vitro*, and even more so *in vivo*.

A prominent inhibition of distal apical dendritic excitation in CA1 is mediated by oriens lacunosum-moleculare (OLM) interneurons activated primarily by CA1 pyramidal cell firing (Gulyas et al., 1993; Blasco-Ibáñez and Freund, 1995). OLM interneurons induced a distal apical dendritic inhibition mediated by both pre- and postsynaptic GABA$_B$R activity in addition to postsynaptic GABA$_A$R activity (Yanovsky et al., 1997), consistent with the wide range of IPIs (30—400 ms) that showed CA3—MPP paired-pulse inhibition in the present study. Paired-pulse inhibition at short intervals (<100 ms) likely involves postsynaptic GABA$_A$ receptors (Steffensen and Henriksen, 1991). In this study, we have provided original evidence that the heterosynaptic CA3-inhibition of the distal dendrites at long intervals (150—400 ms) involves GABA$_B$Rs (Fig. 6), extending previous reports showing similar CA3 inhibition on the mid- and proximal dendrites of CA1 pyramidal cells (Tsai and Leung, 2006; Olpe et al., 1993; Isaacson et al., 1993; Leung et al., 2008). The suppression of the MPP-evoked distal dendritic sink only with high-intensity CA3 conditioning stimulus (Fig. 5B1), and not with MPP conditioning stimulus (Fig. 4C), is consistent with the involvement of OLM interneurons which are activated strongly by firing of CA1 pyramidal cells, while other dendritic inhibiting interneurons are mainly activated by feedforward inhibition (Klausberger and Somogyi, 2008).

Alterations in GABA$_B$R function have been found in TLE and epilepsy models. GABA$_B$R1 polymorphism is associated with TLE (Gambardella et al., 2003). Kindling (Asprodini et al., 1992; Poon et al., 2006) and status epilepticus models resulted in a decrease in GABA$_B$R function (Mangan and Lothman, 1996; Chandler et al., 2003; Straessle et al., 2003), which was suggested to contribute to seizure susceptibility. Additionally, GABA$_B$R1 knockout mice developed spontaneous seizures (Bettler et al., 2004), and acute GABA$_B$R blockade increased partial seizure susceptibility in animals (Leung et al., 2005).

Significance and implications of results

The present data add to a growing body of literature suggesting that early-life seizure activity could have long-lasting effects on brain physiology and function. Reduction in apical dendritic inhibition in CA1 may result in a loss of behavioral function of the hippocampus. In particular, a loss of distal dendritic inhibition in seizure rats may affect spatial coding by a direct entorhinal to CA1 distal-dendritic excitation (Brun et al., 2008; Leung, 2011). Abnormal place cell activity was found in animals with early-life seizures (Dube et al., 2009, 2010). Attenuation in GABA$_B$R function may be a critical component of epilepsy, and it may participate in a role of ''seizures beget seizures'' (Tsai et al., 2008).

Acknowledgement

References

Ang, C.W., Carlson, G.C., Coulter, D.A., 2006. Massive and specific dysregulation of direct cortical input to the hippocampus in temporal lobe epilepsy. J. Neurosci. 26, 11850—11856.

Annegers, J.F., Hauser, W.A., Shirts, S.B., Kurland, L.T., 1987. Factors prognostic of unprovoked seizures after febrile convulsions. N. Engl. J. Med. 316, 493—498.

Asprodini, E.K., Rainnie, D.G., Shinnick-Gallagher, P., 1992. Epileptogenesis reduces the sensitivity of presynaptic gamma-aminobutyric acid B receptors on glutamatergic afferents in the amygdala. J. Pharmacol. Exp. Ther. 262, 1011—1021.

Baram, T.Z., Gerth, A., Schultz, L., 1997. Febrile seizures: an appropriate-aged model suitable for long-term studies. Dev. Brain Res. 98, 265—270.

Berg, A.T., Shinnar, S., 1997. Do seizures beget seizures? An assessment of the clinical evidence in humans. J. Clin. Neurophysiol. 14, 102—110.

Berg, A.T., Shinnar, S., Darefsky, A.S., Holford, T.R., Shapiro, E.D., Salomon, M.E., Crain, E.F., Hauser, A.W., 1997. Predictors of recurrent febrile seizures: a prospective cohort study. Arch. Pediatr. Adolesc. Med. 151, 371—378.

Bettler, B., Kaupmann, K., Mosbacher, J., Gassmann, M., 2004. Molecular structure and physiological functions of GABA$_B$ receptors. Physiol. Rev. 84, 835—867.

Blasco-Ibáñez, J.M., Freund, T.F., 1995. Synaptic input of horizontal interneurons in stratum oriens of the hippocampal CA1 subfield: structural basis of feed-back activation. Eur. J. Neurosci. 7, 2170—2180.

Brun, V.H., Leutgeb, S., Wu, H.Q., Schwarcz, R., Witter, M.P., Moser, E.I., Moser, M.B., 2008. Impaired spatial representation in CA1 after lesion of direct input from entorhinal cortex. Neuron 57, 290—302.

Buckmaster, P.S., Schwartzkroin, P.A., 1995. Interneurons and inhibition in the dentate gyrus of the rat in vivo. J. Neurosci. 15, 774—789.

Chandler, K.E., Princivalle, A.P., Fabian-Fine, R., Bowery, N.G., Kullmann, D.M., Walker, M.C., 2003. Plasticity of GABA(B) receptor-mediated heterosynaptic interactions at mossy fibers after status epilepticus. J. Neurosci. 23, 11382—11391.

Chang, Y.-C., Huang, A.-M., Kuo, Y.-M., Wang, S.-T., Chang, Y.-Y., Huang, C.-C., 2003. Febrile seizures impair memory and cAMP response-element binding protein activation. Ann. Neurol. 54, 706—718.

Chen, K., Baram, T.Z., Soltesz, I., 1999. Febrile seizures in the developing brain result in persistent modification of neuronal excitability in limbic circuits. Nat. Med. 5, 888—894.

Chen, K., Aradi, I., Thon, N., Eghbal-Ahmadi, M., Baram, T.Z., Soltesz, I., 2001. Persistent modified h-channels after complex febrile seizures convert the seizure-induced enhancement of inhibition to hyperexcitability. Nat. Med. 7, 331—337.

Dube, C., Chen, K., Eghbal-Ahmadi, M., Brunson, K., Soltesz, I., Baram, T.Z., 2000. Prolonged febrile seizures in the immature rat model enhance hippocampal excitability long term. Ann. Neurol. 47, 336—344.

Dube, C., Zhou, J.-L., Hamamur, a.M., Zhao, Q., Rinig, A., Abrahams, B.S., McIntyre, K., Nalcioglu, O., Shatskih, T., Baram, T.Z., Holmes, G.L., 2009. Cognitive dysfunction after experimental febrile seizures. Exp. Neurol. 215, 167—177.

Dube, C.M., Ravizza, T., Hamamura, M., Zha, Q., Keebaugh, A., Fok, K., Andres, A.L., Nalcioglu, O., Obenaus, A., Vezzani, A., Baram, T.Z., 2010. Epileptogenesis provoked by prolonged experimental febrile seizures: mechanisms and biomarkers. J. Neurosci. 30, 7484—7494.

Falconer, M.A., 1974. Mesial temporal (Ammon's horn) sclerosis as a common cause of epilepsy. Aetiology, treatment, and prevention. Lancet 2, 767—770.

Freeman, J.A., Nicholson, C., 1975. Experimental optimization of current source-density technique for anuran cerebellum. J. Neurophysiol. 38, 369—382.

Freund, T.F., Buzsaki, G., 1996. Interneurons of the hippocampus. Hippocampus 6, 347—470.

Gambardella, A., Manna, I., Labate, A., Chifari, R., La Russa, A., Serra, P., Cittadella, R., Bonavita, S., Andreoli, V., Lepiane, E., Sasanelli, F., Di Costanzo, A., Zappia, M., Tedeschi, G., Aguglia, U., Quattrone, A., 2003. GABA(B) receptor 1 polymorphism (G1465A) is associated with temporal lobe epilepsy. Neurology 60, 560—563.

Gulyas, A.I., Miles, R., Sik, A., Toth, K., Tamamaky, N., Freund, T.F., 1993. Hippocampal pyramidal cells excite inhibitory neurons through a single release site. Nature 366, 683—687.

Hara, K., Harris, R.A., 2002. The anesthetic mechanism of urethane: the effects on neurotransmitter-gated ion channels. Anesth. Analg. 94, 313—318.

Isaacson, J.S., Solis, J.M., Nicoll, R.A., 1993. Local and diffuse synaptic actions of GABA in the hippocampus. Neuron 10, 165—175.

Klausberger, T., Somogyi, P., 2008. Neuronal diversity and temporal dynamics: the unity of hippocampal circuit operations. Science 321, 53—57.

Leung, L.S., 2010. Field potential generation and current source density analysis. In: Vertes, R.P., Stackman, R.W. (Eds.), NeuroMethods, vol. 15. Humana Press, Clifton, NJ, pp. 1—26.

Leung, L.S., 2011. A model of intracellular theta phase precession dependent on intrinsic subthreshold membrane currents. J. Neurosci. 31, 12282—12296.

Leung, L.S., Peloquin, P., 2006. GABA$_B$ receptors inhibit backpropagating dendritic spikes in hippocampal CA1 pyramidal cells in vivo. Hippocampus 16, 388—407.

Leung, L.S., Canning, K.J., Shen, B., 2005. Hippocampal afterdischarges after GABA$_B$ receptor blockade in the behaving rat. Epilepsia 46, 203—216.

Leung, L.S., Peloquin, P., Canning, K.J., 2008. Paired-pulse depression of excitatory postsynaptic current sinks in hippocampal CA1 in vivo. Hippocampus 18, 1008—1020.

Leung, L.S., Roth, L., Canning, K.J., 1995. Entorhinal inputs to hippocampal CA1 and dentate gyrus in the rat: a current-source-density study. J. Neurophysiol. 73, 2392—2403.

Maher, J., McLachlan, R.S., 1995. Febrile convulsions. Is seizure duration the most important predictor of temporal lobe epilepsy? Brain 118, 1521—1528.

Mangan, P.S., Lothman, E.W., 1996. Profound disturbances of pre- and postsynaptic GABAB-receptor-mediated processes in region CA1 in a chronic model of temporal lobe epilepsy. J. Neurophysiol. 76, 1282—1296.

Nelson, K.B., Ellenberg, J.H., 1978. Prognosis in children with febrile seizures. Pediatrics 61, 720—727.

Olpe, H.R., Steinmann, M.W., Ferrat, T., Pozza, M.F., Greiner, K., Brugger, F., Froestl, W., Mickel, S.J., Birtiger, H., 1993. The actions of orally active GABA$_B$ receptor antagonists on GABAergic transmission in vivo and in vitro. Eur. J. Pharmacol. 233, 179—186.

Paxinos, G., Watson, C., 1986. The Rat Brain in Stereotaxic Coordinates, 2nd ed. Academic Press, New York.

Poon, N., Kloosterman, F., Wu, C., Leung, L.S., 2006. Presynaptic GABA$_B$ receptors on glutamatergic terminals of CA1 pyramidal cells decrease in efficacy after partial hippocampal kindling. Synapse 59 (3), 125—134.

Steffensen, S.C., Henriksen, S.J., 1991. Effects of baclofen and bicuculline on inhibition in the fascia dentata and hippocampus regio superior. Brain Res. 538, 46—53.

Straessle, A., Loup, F., Arabadzisz, D., Ohning, G.V., Fritschy, J.M., 2003. Rapid and long term alterations of hippocampal GABAB receptors in a mouse model of temporal lobe epilepsy. Eur. J. Neurosci. 18, 2213—2226.

Tsai, M.L., Leung, L.S., 2006. Decrease of hippocampal GABA$_B$ receptor-mediated inhibition after hyperthermia-induced seizures in immature rats. Epilepsia 47, 277—287.

Tsai, M.L., Shen, B., Leung, L.S., 2008. Seizures induced by GABA$_B$ receptor blockade in early-life induced long-term GABA$_B$ receptor hypofunction and kindling facilitation. Epilepsy Res. 79, 187—200.

Verity, C.M., Golding, J., 1991. Risk of epilepsy after febrile convulsions: a national cohort study. Br. Med. J. 303, 1373—1376.

Verity, C.M., Greenwood, R., Golding, J., 1998. Long-term intellectual and behavioral outcomes of children with febrile convulsions. N. Engl. J. Med. 338, 1723—1728.

Wu, K., Leung, L.S., 2003. Increased dendritic excitability in hippocampal CA1 in vivo in the kainic acid model of temporal lobe epilepsy: a study using current source density analysis. Neuroscience 116, 599—616.

Yanovsky, Y., Sergeeva, O.A., Freund, T.F., Haas, H.L., 1997. Activation of interneurons at the stratum oriens/alveus border suppresses excitatory transmission to apical dendrites in the CA1 area of the mouse hippocampus. Neuroscience 77, 87—96.